Comparative Biochemistry and Physiology, Part B 191 (2016) 36–45

Contents lists available at ScienceDirect

Comparative Biochemistry and Physiology, Part B

journal homepage: www.elsevier.com/locate/cbpb

Claudin gene expression patterns do not associate with interspecific differences in paracellular nutrient absorption

Edwin R. Price [a,*], Katherine H. Rott [a], Enrique Caviedes-Vidal [b,c], William H. Karasov [a]

[a] Department of Forest and Wildlife Ecology, University of Wisconsin-Madison, Madison, WI 53706, USA
[b] Departamento de Bioquímica y Ciencias Biológicas y Laboratorio de Biología "Profesor E. Caviedes Codelia", Universidad Nacional de San Luis, 5700 San Luis, Argentina
[c] Laboratorio de Biología Integrativa, Instituto Multidisciplinario de Investigaciones Biológicas de San Luis, Consejo Nacional de Investigaciones Científicas y Técnicas, 5700 San Luis, Argentina

ARTICLE INFO

Article history:
Received 30 March 2015
Received in revised form 8 September 2015
Accepted 9 September 2015
Available online 21 September 2015

Keywords:
Intestine
Occludin
Paracellular absorption
Tight junction
Comparative transcriptomics

ABSTRACT

Bats exhibit higher paracellular absorption of glucose-sized molecules than non-flying mammals, a phenomenon that may be driven by higher permeability of the intestinal tight junctions. The various claudins, occludin, and other proteins making up the tight junctions are thought to determine their permeability properties. Here we show that absorption of the paracellular probe L-arabinose is higher in a bat (*Eptesicus fuscus*) than in a vole (*Microtus pennsylvanicus*) or a hedgehog (*Atelerix albiventris*). Furthermore, histological measurements demonstrated that hedgehogs have many more enterocytes in their intestines, suggesting that bats cannot have higher absorption of arabinose simply by having more tight junctions. We therefore investigated the mRNA levels of several claudins and occludin, because these proteins may affect permeability of tight junctions to macronutrients. To assess the expression levels of claudins per tight junction, we normalized the mRNA levels of the claudins to the constitutively expressed tight junction protein ZO-1, and combined these with measurements previously made in a bat and a rodent to determine if there were among-species differences. Although expression ratios of several genes varied among species, there was not a consistent difference between bats and non-flyers in the expression ratio of any particular gene. Protein expression patterns may differ from mRNA expression patterns, and might better explain differences among species in arabinose absorption.

1. Introduction

In the intestine, adjacent enterocytes are linked by tight junctions, which impede the movement of molecules across the epithelium and thereby form a barrier to solute flux. Tight junctions are complex structures composed of proteins such as claudins and occludin (OCLN) that span the cell membrane and interact in the extracellular space between cells, and also connect with intracellular scaffolding proteins via interactions with zonula occludens 1 (ZO-1) (Shen et al., 2011). These several proteins are thought to mediate the permeability characteristics of tight junctions, determining for example, the size and charge of solutes that can pass through the tight junction (Günzel and Yu, 2013). Many studies of tight junctions have focused on the movement of ions across the epithelium, although a few have investigated the permeability to larger, macronutrient-sized molecules. For example, overexpression and deletion studies of OCLN and claudin-1 (CLDN1) have shown that these genes are associated with increased permeability to mannitol (McCarthy et al., 2000; Van Itallie et al., 2001; Amasheh et al., 2002; Tamura et al., 2011), although this is not a consistent finding across all studies (see for example Schulzke et al., 2005). The effects of altered expression of any tight junction protein may be context-specific (depending on starting expression level, expression of other proteins, tissue type, etc.), and it is still not certain whether any claudins affect the permeability to macronutrients in a specific way (Günzel and Yu, 2013).

Variation in tight junction permeability might be able to provide a mechanistic explanation for the variation among species in their reliance on paracellular nutrient absorption. Whereas non-flying mammals such as rodents rely heavily on the transcellular, transporter-mediated pathway of glucose absorption, small birds and bats use the paracellular pathway (i.e., movement of glucose through tight junctions) for a majority of glucose absorption (Caviedes-Vidal et al., 2007; Karasov et al., 2012; Brun et al., 2014; Price et al., 2014). This has been hypothesized to help birds and bats compensate for their smaller intestines (Caviedes-Vidal et al., 2007; Price et al., 2015).

Although high paracellular glucose absorption has been documented in all bat species studied (Keegan, 1980, 1984; Tracy et al., 2007; Caviedes-Vidal et al., 2008; Fasulo et al., 2013a; Brun et al., 2014; Price et al., 2014), the mechanism by which this occurs is still unclear. Bats might simply have more tight junctions in their intestines, achieved either by greater villous amplification or smaller enterocytes. Alternatively, bats might have tight junctions that are more permeable to macronutrient-sized molecules. We recently suggested that both may be occurring

* Corresponding author at: Department of Biological Sciences, 1511 W. Sycamore, Denton, TX 76203, USA. Tel.: +1 608 234 2665; fax: +1 940 565 3821.
E-mail address: Edwin.price@unt.edu (E.R. Price).

http://dx.doi.org/10.1016/j.cbpb.2015.09.003
1096-4959/

(Price et al., 2014). Little brown bats (*Myotis lucifugus*) have a higher density of cells (and presumably tight junctions) than white-footed mice (*Peromyscus leucopus*), but the total number of enterocytes in the small intestine was lower. We suggested that the higher paracellular absorption of nutrients by little brown bats must instead be driven by characteristics of the tight junction, and we demonstrated differences in tight junction gene expression between the species. In particular, expression levels of CLDN1 and CLDN15 were higher, and the expression level of CLDN2 was lower, in little brown bat intestine compared to the white-footed mouse (Price et al., 2014).

This single species-pair comparison was intriguing, but begs further testing. For example, some of those expression differences might be related more to diet, phylogeny, or mere chance, than to the intestinal permeability characteristics associated with those species. In the present study, we therefore made integrated measurements on 3 more species: the insectivorous big brown bat (*Eptesicus fuscus*), the herbivorous meadow vole (*Microtus pennsylvanicus*), and the insectivorous hedgehog (*Atelerix albiventris*). These species provide a new comparison of a bat and a rodent, and the hedgehog provides a non-flying species that not only shares an insectivorous diet with the bat, but as part of the Laurasiatheria, is more closely related to the bat than to the vole (Nery et al., 2012). First, we demonstrate that the big brown bat has higher paracellular absorption of glucose-sized molecules than the non-flying species, thus confirming the pattern of high paracellular permeability in bats. Next we examine the anatomy and histology of the intestine, and show that it is unlikely that the high paracellular permeability in the bat can be explained by simply having more tight junctions than non-flyers. Finally, we measured tight junction gene expression in an attempt to understand how claudins and OCLN control paracellular permeability to glucose. For these gene expression measurements, we make comparisons among these three species and also with two previously measured species, the little brown bat (*M. lucifugus*) and the white-footed mouse (*P. leucopus*) (Price et al., 2014).

2. Methods

2.1. Animals

Big brown bats (*E. fuscus*) are common North American insectivorous bats (Kurta and Baker, 1990) (Table 1). We captured them in Dane County, Wisconsin, using mistnets placed near streams or over the exit of bats' day roosts in human habitations. Bats were used in experiments immediately following capture. We obtained domesticated hedgehogs (*A. albiventris*, all over 6 months age) from breeders in Wisconsin. Hedgehogs (order Erinaceomorpha) are primarily insectivorous (Santana et al., 2010), and were maintained on a diet of Purina Cat Chow Complete supplemented occasionally with mealworms (larvae of *Tenebrio molitor*). They were kept under 12 h:12 h L:D lighting conditions with food and water provided ad libitum between experiments. Meadow voles (*M. pennsylvanicus*) are common grassland rodents of the Midwest and northeastern United States and have a primarily herbaceous diet (Lindroth and Batzli, 1984). We captured meadow voles in the Biocore Prairie and community gardens of the Lakeshore Nature Preserve, University of Wisconsin-Madison. Voles were maintained under similar conditions as the hedgehogs except that their diet consisted of a commercial rodent chow (Purina 5010 Rodent Diet) supplemented daily with fresh produce (kale, carrots, and apples). No animals were obviously pregnant at the time of capture or testing. The sample sizes in Table 1 are for gene expression measurements. Smaller subsets of animals (noted in other tables and figures) were used for whole-animal and histology measurements so as to conserve resources. Experiments were approved by the University of Wisconsin-Madison Animal Care and Use Committee (#A1441). Bats and voles were caught with permission from the Wisconsin Department of Natural Resources (permits E/T 704 and SCP-SOD-2011).

Table 1
Animal attributes and gut measurements.

	Eptesicus fuscus	*Atelerix albiventris*	*Microtus pennsylvanicus*
N (#♂/#♀)	5/6	0/6	7/2
Body mass (g)	17.9 ± 1.1	439 ± 33	35.4 ± 4.1
Body length (cm; snout to base of tail)	7.1 ± 0.2	18.8 ± 0.8	10.86 ± 0.5
Small intestine length (cm)	12.4 ± 0.6[a]	54.1 ± 3.6[a]	26.3 ± 1.3
Small intestine circumference (mm)	6.58 ± 0.22	11.06 ± 0.19	7.59 ± 0.33
Cecum mass (g wet; including contents)	Absent	Absent	1.75 ± 0.17
Large intestine length (cm)	n.m.[a]	n.m.[a]	11.6 ± 0.73

[a] n.m. = not measured. In *E. fuscus* and *A. albiventris*, the large intestine is short and difficult to distinguish from the small intestine macroscopically. For these animals, the small intestine length listed in this table is the length of the whole intestine.

2.2. Measurement of paracellular nutrient absorption

We used two radiolabeled probes to assess nutrient absorption. L-arabinose (M_r 150) is a carbohydrate that is somewhat smaller than D-glucose (M_r 180) but its absorption is not transporter-mediated in bats or rodents (Lavin et al., 2007; Price et al., 2014). Its absorption was therefore used as an estimate of the paracellular component of D-glucose absorption. The difference between arabinose and glucose in molecular size likely causes this to be an overestimation, a point we consider further in our discussion. To estimate total glucose absorption, we used 3-O-methyl-D-glucose (3OMD-glucose), a molecule that is absorbed by both mediated and non-mediated mechanisms like D-glucose, but unlike glucose, is not substantially metabolized, and thus can be readily recovered. In the non-flying species, we also measured absorption of lactulose (M_r 342) and creatinine (Mr 113), and we present those data in Supplementary Table S1. Creatinine and lactulose absorptions were not assessed in the big brown bats due to a scarcity of experimental animals of that species.

Animals were dosed orally with [^{14}C]-L-arabinose and [^{3}H]-3OMD-glucose at the same time. The gavage vehicle was 50 mM glucose in water. Although Na^+ is required for Na^+-coupled glucose transport, Na^+ is secreted into the gut with bicarbonate and can readily diffuse from the blood (Brody, 1999). Thus, the lack of sodium in the gavage solution should not have affected our results, and indeed, glucose absorption was complete (see Results). After dosing, animals were placed in a metabolic chamber for collection of urine over the following several hours, where they had access to 50 mM glucose in water but no food. Voles and hedgehogs were placed in standard rat-sized wire-bottomed metabolic chambers, but for hedgehogs, we modified the chamber to have a smaller (5.7 mm) mesh size which seemed to make walking around the cage easier and more comfortable. Previously, we have favored a serial blood sampling technique in bats because of the difficulty of collecting urine (and separating it from feces) in bats (Tracy et al., 2007; Caviedes-Vidal et al., 2008; Brun et al., 2014). However, we tested and adopted a urine collection technique for bats in this study. We designed a small (15 × 15 × 5 cm) plastic metabolic chamber with metal screening glued to the top from which the bats could easily hang, and a sealable door near the bottom through which we could collect urine. The bats rarely produced feces during the experiments, and it was generally easy to separate from urine. Bats were occasionally offered water with or without glucose using a ball-tipped syringe, although they rarely drank. There were few urination events, and this likely led to some experimental variation, but this technique had some advantages over blood collection: 1) we were able to use the same calculation of fractional absorption for bats and the non-flying species, 2) we could avoid taking multiple blood samples from a small animal, and therefore, 3) we were able to use fewer bats because we could conduct two separate trials on individual bats.

In separate trials, we injected the same probes intraperitoneally (saline vehicle) and collected urine in a similar manner. Urine subsamples were counted with a Wallac 1414 liquid scintillation counter (PerkinElmer, Waltham, MA, USA). Fractional absorption (f) of probes was determined by dividing the recovery (percentage of dose recovered in urine) in gavage trials by the recovery in injection trials. We found that we achieved asymptotic recovery of probes within about 3 h in bats. We therefore waited at least 6 h between trials in bats to provide an extra buffer period, and we also alternated the order of injection and gavage for the various bats to control for any potential carryover effects. In the non-flying species, trials were separated by at least 3 days.

2.3. Tissue histology

Following the absorption trials, we euthanized the animals with isofluorane anesthesia and pneumothorax. The small intestine was removed, measured for length, divided into thirds, cut longitudinally, and laid flat to measure circumference using calipers. From each third, we preserved a central 2-cm segment in 10% formalin. At this time, we also placed in RNAlater a small segment from the distal end of the proximal third (see Gene expression). Later, 5-μm sections were cut and stained with hematoxylin and eosin. We measured villus length, villus width, and crypt width using 200× magnification and counting 25 villi per section using NIS-Elements D software (Nikon Instruments, Melville, NY). We then calculated amplification ratio according to Kisielinski et al. (2002).

We measured enterocyte size by counting the number of enterocytes per length along a villus (10 villi per section) at 400× magnification. The inverse of this measurement is the average width of an enterocyte. Enterocyte width was squared to determine the lumenal surface area of an average enterocyte, and we multiplied this by the villous amplification ratio to determine the number of enterocytes per nominal surface area. For each section, this was multiplied by nominal surface area to determine the number of enterocytes per section, and sections were summed to calculate the total number of enterocytes in the intestine.

2.4. Gene expression

We determined mRNA expression profiles for several tight junction-associated genes that are expressed in the intestine (ZO-1, OCLN, CLDN1, CLDN2, CLDN4, CLDN7, and CLDN15) in 11 *E. fuscus*, 6 *A. albiventris*, and 9 *M. pennsylvanicus*. We also measured the expression of two common housekeeper genes (RPLP0 and EEF1A1). Tissue that had been stored in RNAlater was extracted using TRIzol (Life Technologies, Carlsbad, CA). RNA concentration was determined from absorbance at 260 nm using a NanoDrop spectrophotometer (Thermo Scientific, Wilmington, DE), and purity was checked by the A_{260}/A_{280} ratio (≈2 for all samples). 10 μg RNA was digested using DNase I (New England Biolabs, Ipswich, MA) to remove genomic DNA, and RNA was then reverse transcribed to cDNA (iScript cDNA synthesis kit, Bio-Rad, Hercules, CA).

Degenerate primers were designed using known or predicted sequences for mammals in GenBank (Benson et al., 2012) and were used to determine partial coding sequences for our target genes. Specific primer sets were then designed with the aid of computer programs (Rozen and Skaletsky, 2000; Larkin et al., 2007) (Table 2). We verified that specific primers amplified a single target by examination of melt curves, the presence of a single band when the product is electrophoresed, and subsequent sequencing of that band.

For the best comparisons across species, we sought to design specific primers that amplified the target genes in all 3 species. This should make it likely that the amplification efficiency is similar across species. Further, it should make the fluorescence per amplicon (which varies with amplicon length) similar across species. However, for most genes, the sequences varied too much among species to design a single set of primers that would amplify in all 3 species. Additionally, we wished to make comparisons with data from 2 previously reported species (the little brown bat, *M. lucifugus*, n = 9; and the white-footed mouse, *P. leucopus*, n = 8) (Price et al., 2014), in which amplicon length sometimes differed substantially from the present study. We therefore accounted for differences among species in the following additional two ways.

First, we used LinRegPCR (Ruijter et al., 2009) for calculation of starting concentrations. The LinRegPCR algorithm uses the log-linear amplification phase to calculate efficiency for each sample. We could therefore obtain many semi-independent estimates of amplification efficiency for each gene in each species. As recommended by the program designers (Ruijter et al., 2009), for each gene (i.e., for each amplicon), we averaged the efficiency for each species and applied that average to the calculation for that gene for every sample within the species. Reaction efficiency exceeded 1.75 for all genes in all species. For each gene, we chose a fluorescence threshold that was common to all 5 species (including the 2 previously reported (Price et al., 2014)) before calculating the starting concentration.

Table 2
Primers used for qPCR and the GenBank accessions upon which they were based[a].

Gene	Forward primer (5′ to 3′)	Reverse primer (5′ to 3′)	GenBank accessions
Zonula occludens 1 (ZO-1)	*M. pennsylvanicus* and *A. albiventris*: CGTAGCTCTGGCATTATTCG *E. fuscus*: CGTAGCTCCGGCATCATCCG	*M. pennsylvanicus* and *A. albiventris*: CCTGGCACTTTTCCGAGA *E. fuscus*: CCTGGCACTCTTCCGAGA	KJ420409–KJ420412
Occludin (OCLN)	*M. pennsylvanicus*: ATCCTGGGCATCCTGGTGT *A. albiventris*: GTCCTGGGCATTATGGTGTT *E. fuscus*: ATCCTGGGCTTCATGGTGTT	All 3 species: GGGATCCACCACACAGTAGT	KJ451437–KJ451442
Claudin-1 (CLDN1)	*E. fuscus* and *A. albiventris*: TGCGGATGGCTGTCATTG *M. pennsylvanicus*: TGTGGATGGCTGTCATTG	All 3 species: CAGCCCAGCCAGTGAAGAG	KJ420416–KJ420420
Claudin-2 (CLDN2)	*M. pennsylvanicus* and *A. albiventris*: CAAGTTCTTATGTTGGTGCCAGC *E. fuscus*: CAAGTTCTTATGTTGGTGCTAGC	*M. pennsylvanicus* and *A. albiventris*: CTGGGCAGCCTGGATGT *E. fuscus*: CTGAGCAGCCTGGATGT	KJ451447–KJ451450
Claudin-4 (CLDN4)	All 3 species: AACTGCGTGGTGCAGAGC	*E. fuscus* and *M. pennsylvanicus*: GCAGTTGGTGCACTTGCC *A. albiventris*: GCAGTTGGTACATTTGCC	KJ406716–KJ406719
Claudin-7 (CLDN7)	All 3 species: TACGACTCGGTGCTCGC	All 3 species: AGCAAGACCTGCCACGAT	KJ451444–KJ451446
Claudin-15 (CLDN15)	*M. pennsylvanicus*: GGAGTTCCCTTCCATGCT *E. fuscus*: GGAGTTCCCGTCCATGCT *A. albiventris:* CGAGTTCCCGTCCCTGC	*M. pennsylvanicus* and *E. fuscus*: CCAGGAAGCCCAGGAGG *A. albiventris*: CCAGACCGCCCATCAG	KJ502667–KJ502669
EEF1A1	All 3 species: CAGCACCTACATTAAGAAAATTGG	All 3 species: CCCTTGAACCAAGGCATATT	KJ396960–KJ396962
RPLP0	All 3 species: GCGACCTGGAAGTCCAACTA	All 3 species ATCTGCTGCATCTGCTTGG	KJ396955–KJ396959

[a] Primers and accession numbers for *M. lucifugus* and *P. leucopus* can be found in Price et al. (2014).

Secondly, we corrected for differences in fluorescence per amplicon by dividing the starting concentration (calculated above) by the amplicon length (see mathematical derivation in Appendix A). Because we amplified similar sections of the genes in the various species, this correction was generally small (coefficients of variation ranging 0–1%, depending on the gene). However, comparing to our previous study where amplicons were often of different lengths, the correction could be substantially greater (CVs: 0–37%).

In order to examine the composition of the tight junctions, we calculated expression ratios of 2 tight junction genes, thus controlling for the number of tight junctions. The expression ratios we report here are calculated as: (corrected starting concentration of the target gene) / (corrected starting concentration of the denominator gene). Although 2 standard housekeeper genes (EEF1A1 and RPLP0) were available to us, we were concerned that these do not provide appropriate denominators for understanding the composition of tight junctions. This is because whole tissue was used for extractions, and the species may differ in the ratio of enterocytes to other cells (e.g., muscle and connective tissue) in the intestinal samples. A ratio of CLDN2 to EEF1A1 expression, for example, might be informative about interspecific differences in the amount of CLDN2 or the number of tight junctions per mass of intestine, but will not necessarily be informative regarding the compositional makeup of each tight junction, the variable of interest in this study. Similarly, the ratio of a claudin gene to standard housekeepers might be driven by the total number of tight junctions per enterocyte, and not by the composition of the tight junction per se. Ultimately, we wanted to assess the compositional makeup of claudins per tight junction, and therefore we needed to use a gene that is specific to tight junctions in the denominator of the expression ratio. This has the effect of controlling for the total number of tight junctions. Because ZO-1 is thought to be constitutively expressed in tight junctions (Holmes et al., 2006), we preferred ZO-1 as this denominator gene. Obviously, this choice could affect our results if the species vary in the amount of ZO-1 expressed per tight junction. Therefore we also investigated the use of other tight junction genes as well as more standard housekeeper genes (RPLP0 and EEF1A1) in the denominator of the expression ratios. The consequences of this choice are addressed further in the discussion.

We used Platinum Taq polymerase (Life Technologies; conditions: 1× buffer, 2.5 mM MgCl2, 0.2 mM dNTPs, 0.25 μM each primer, 1 unit Taq, 0.7× SYBR Green 1, 1 μl template in 20 μl rxn volume). We ran samples in duplicate with a cycling program of 94 °C for 10 min, then 40 cycles of 94 °C for 30 s, 55 °C for 30 s, and 72 °C for 30 s, with fluorescence acquisition at the end of the 72 °C step.

2.5. Statistics

Differences among species were detected using ANOVA and Tukey's post-hoc tests. Significance was set at $P < 0.05$. Tests were performed with the aid of R software (R Development Core Team, 2010). Principal components analysis was performed in R using expression ratios. When data were missing for the principal components analysis, we imputed data based on species averages, or variable averages when that was not available. Data are presented as means + SE.

3. Results

3.1. Absorption of paracellular probes in intact animals

Absorption of 3OMD-glucose was essentially complete (*f* not significantly different from unity) in the bat and the vole ($P > 0.6$ for both) (Fig. 1). There was no statistical difference in fractional absorption of 3OMD-glucose among species, but in the hedgehog, 3OMD-glucose absorption was somewhat less than unity ($f = 0.84 \pm 0.05$, $P = 0.021$). In the bat, arabinose absorption was 85 ± 14.2%, which was significantly higher ($F_{2,17} = 8.9$, $P = 0.0025$) than the hedgehog (45 ± 4.7%; $P = 0.037$) or the vole (22 ± 2.3%; $P = 0.0025$) (Fig. 1).

3.2. Morphometry and histology

The bats had shorter intestines than both the voles and hedgehogs ($F_{2,23} = 160$, $P < 0.0001$, $P < 0.0001$) (Table 1). Hedgehogs also had wider intestines than the voles and bats ($F_{2,24} = 94$, $P < 0.0001$; $P < 0.0001$), although intestinal circumference was not significantly different between the voles and bats ($P = 0.17$) (Table 1).

Due to their longer villi, hedgehogs had the highest amplification ratio of the 3 species (Table 3) (Fig. 2). Enterocyte width was somewhat lower in the bats compared to the two non-flying species, and the bat had more enterocytes per nominal surface area than the vole. However, due largely to their longer intestines, voles and hedgehogs had a much greater number of cells (and thus tight junctions) summed over the small intestine (Table 3). The nominal surface area of vertebrates scales with (body mass)$^{0.76}$ (Karasov, 2012). If we correct for this scaling relationship, the bats have summed nominal surface areas (0.92 ± 0.4 cm^2 g$^{-.76}$) ($F_{2,23} = 10.4$, $P = 0.0005$) that are lower than voles (1.36 ± 0.17 cm^2 g$^{-.76}$) ($P = 0.012$) and not significantly different from hedgehogs (0.59 ± 0.02 cm^2 g$^{-.76}$) ($P = 0.14$). Similarly we can calculate the number of cells per normalized nominal surface area by dividing the number of cells in the intestine by (body mass)$^{0.76}$. The bats had significantly higher ($F_{2,8} = 5.6$, $P = 0.03$) total cells per intestine normalized for body mass (25 ± 3 million cells g$^{-.76}$) than the voles (17 ± 1 million cells g$^{-.76}$; $P = 0.03$) but not hedgehogs (22 ± 2 million cells g$^{-.76}$; $P = 0.55$).

3.3. RNA expression

We tried several ways of calculating the expression ratio, i.e., the ratio of the target gene divided by a denominator gene. As we note in the methods, we prefer using ZO-1 as the denominator gene, because it: 1) is thought to be expressed constitutively in the tight junctions; 2) could be measured in all species and therefore can be used to construct an expression ratio in all species; and 3) is a gene associated with the tight junction, and therefore, using it in the denominator provides a measure of the relative expression of the target gene while controlling for the total number of tight junctions, which may vary among species. The following results are based on using ZO-1 as the denominator gene, but we also show the results expressed using other denominator genes (Supplementary Figs. S1–S7).

The CLDN1 expression ratio varied among species ($F_{3,33} = 2.9$, $P = 0.0474$) (Fig. 3). The expression ratio in *P. leucopus* was significantly lower than in *E. fuscus* ($P = 0.041$). The CLDN2 expression ratio also varied significantly among species ($F_{3,32} = 5.1$, $P = 0.0053$), being significantly lower in *M. lucifugus* ($P = 0.003$) compared to *E. fuscus*. The

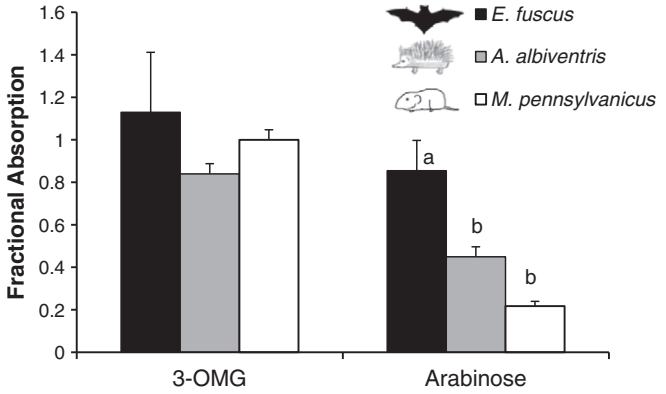

Fig. 1. Fractional absorption of a glucose analog (3-O-methyl-D-glucose; 3-OMG) and a paracellularly absorbed probe (L-arabinose) in 8 big brown bats (*Eptesicus fuscus*), 6 hedgehogs (*Atelerix albiventris*), and 5 meadow voles (*Microtus pennsylvanicus*). Fractional absorption is calculated as oral bioavailability, and represents the proportion of an oral dose that is absorbed by the animal. Fractional absorption of L-arabinose was significantly higher in the bat than either of the non-flying mammals. Data are means + SE.

Table 3
Histological measurements from small intestine of big brown bats (*Eptesicus fuscus*), meadow voles (*Microtus pennsylvanicus*) and hedgehogs (*Atelerix albiventris*).

	E. fuscus (n = 3)	*M. pennsylvanicus* (n = 5)	*A. albiventris* (n = 6)	F	P-value
Villus length (μm)					
Proximal	571 ± 45[a]	602 ± 44[a]	1220 ± 41[b]	$F_{2,11} = 74$	<0.0001
Medial	445 ± 40[a]	583 ± 27[a]	999 ± 37[b]	$F_{2,11} = 66$	<0.0001
Distal	313 ± 38[a]	432 ± 35[a]	731 ± 63[b]	$F_{2,8} = 20$	0.0008
Villus width (μm)					
Proximal	72 ± 8.0[a]	94 ± 6.6[a]	166 ± 4.9[b]	$F_{2,11} = 64$	<0.0001
Medial	74 ± 5.6[a]	86 ± 2.6[a]	159 ± 4.0[b]	$F_{2,11} = 138$	<0.0001
Distal	73 ± 7.3[a]	77 ± 4.0[a]	134 ± 5.7[b]	$F_{2,8} = 35$	0.0001
Crypt Width (μm)					
Proximal	73 ± 6.9[a]	86 ± 3.3[a,b]	155 ± 1.3[b]	$F_{2,11} = 12$	0.0017
Medial	37 ± 1.8[a]	43 ± 1.7[a]	49 ± 1.4[b]	$F_{2,11} = 14.7$	0.0008
Distal	39 ± 2.3	39 ± 1.3	48 ± 1.2	$F_{2,8} = 0.36$	0.7079
Amplification Ratio					
Proximal	14.8 ± 2.0[a,b]	12.6 ± 0.80[a]	18.0 ± 0.77[b]	$F_{2,11} = 8$	0.0072
Medial	11.0 ± 1.3[a]	13.3 ± 0.48[a,b]	15.2 ± 0.52[b]	$F_{2,11} = 8.7$	0.0054
Distal	8.1 ± 1.1[a]	10.7 ± 0.48[a,b]	13.1 ± 0.90[b]	$F_{2,8} = 9.35$	0.0081
Enterocyte Width (μm)					
Proximal	6.39 ± 0.42[a]	8.33 ± 0.15[c]	7.47 ± 0.11[b]	$F_{2,11} = 20.5$	0.0001
Medial	6.34 ± 0.32[a]	8.23 ± 0.18[c]	7.49 ± 0.12[b]	$F_{2,11} = 21.6$	0.0002
Distal	6.53 ± 0.33[a]	8.14 ± 0.18[b]	7.64 ± 0.04[b]	$F_{2,8} = 14.9$	0.0020
Cells per nominal surface area (10^6 cells per cm^2)					
Proximal	36.2 ± 3.8[a]	18.2 ± 1.0[b]	32 .4 ± 1.7[a]	$F_{2,11} = 22.2$	0.0001
Medial	27.2 ± 0.6[a]	19.7 ± 0.8[b]	27.3 ± 1.6[a]	$F_{2,11} = 10.5$	0.0028
Distal	18.8 ± 1.3[a,b]	16.2 ± 0.8[a]	22.4 ± 1.7[b]	$F_{2,8} = 6.6$	0.0199
Summed cells of the small intestine (10^6 cells)	206 ± 42[a]	308 ± 24[a]	2308 ± 115[b]	$F_{2,8} = 355$	<0.0001

F and P values refer to an ANOVA for differences among species.
Within a row, values that share letters do not differ significantly (P > 0.05) with Tukey's HSD test.

CLDN4 expression ratio did not vary significantly among species ($F_{2,26} = 2.1$, P = 0.14). For CLDNs 1, 2, and 4, we tried two primer sets for the hedgehog (*A. albiventris*) but could not produce suitable melt curves.

The CLDN7 expression ratio varied significantly among species ($F_{4,38} = 12.6$, P < 0.0001), with the bats and mouse tending to display higher expression ratios than the other species. The CLDN15 expression ratio varied significantly among species ($F_{4,38} = 4.6$, P = 0.0039), with *M. lucifugus* displaying higher expression than *M. pennsylvanicus* and *P. leucopus* (P < 0.024 for both). The OCLN expression ratio varied among species ($F_{4,38} = 11.6$, P = 0.0013), with expression in *A. albiventris* and *M. lucifugus* tending to be higher than the rodents (Fig. 3).

Given that we used new correction factors, we were interested in whether the expression patterns we reported previously (Price et al., 2014) changed. Although statistical significance was sometimes lost in the current study, the patterns observed were the same (*M. lucifugus* had lower CLDN2 and higher CLDN1 and CLDN15 expression ratios compared to *P. leucopus*). The loss of significance can likely be attributed to lower statistical power due to the addition of the new species. Regardless of statistical significance, however, the expression differences we previously observed between *M. lucifugus* and *P. leucopus* were not replicated in the 3 new species. The CLDN1 expression ratio, for example, was just as high in *M. pennsylvanicus* as the two bats (Fig. 3). The expression ratio of CLDN2 was relatively high in *E. fuscus*, whereas it was low in *M. lucifugus*. The pattern of differences between bats and rodents for the CLDN15 expression ratio held up in the new analysis, but the hedgehog had a CLDN15 expression ratio that was similar to that of the bats. We also examined our results using different genes in the denominator of the expression ratios (for example EEF1A1, RPLP0, and CLDN genes), but in no case was there a clear difference between bats and non-flyers (Supplementary Figs. S1–S7). Using an average of the expression of EEF1A1 and RPLP0 as the denominator resulted in expression ratios that are qualitatively similar to those using ZO-1 as the denominator (compare Fig. 3 with Fig. S7).

Our principal components analysis found 2 components that together account for 63% of the variance (Table 4). The first PCA axis had high negative loadings for CLDN2 and CLDN4 and a high positive loading for OCLN. The second axis had a strong negative loading for CLDN15 (Table 4). Plotting the individual scores for the first and second axes, the species did not segregate into distinct groups (Fig. 4). The bats tended to have strongly negative PC2 scores, while the vole had positive PC2 scores, although there was substantial overlap among all species (Fig. 4).

4. Discussion

4.1. Paracellular nutrient absorption in intact animals

As we have observed in previous comparisons of bats and rodents (Brun et al., 2014; Price et al., 2014), the big brown bat absorbed the majority of the L-arabinose dose, whereas the vole absorbed only a minority. Although we hasten to point out that we have not performed a fully phylogenetically controlled analysis, the hedgehog, which is more closely related to bats than rodents (Nery et al., 2012), provides extra confidence that, among mammals, the phenomenon of high paracellular absorption of nutrient-sized probes is unique to bats. L-arabinose absorption in the hedgehog (45%) and the vole (22%) were near or within in the range observed previously in rodents (15–40%) (Fasulo et al., 2013b; Price et al., 2013, 2014; Brun et al., 2014). Thus, our results lend further support to the hypothesis that flying vertebrates have evolved high intestinal permeability to nutrients to compensate for their smaller intestines (Caviedes-Vidal et al., 2007; Price et al., 2015). The species in this study varied in their source (wild vs. domestic) and duration in captivity (bats were used immediately after capture). Additionally, the natural and captive diets varied among species. These differences may have affected the animals' stress levels and intestinal function during our experiments. However, the interspecific differences in paracellular nutrient absorption we observed are consistent with those previously observed in other species representing a range of diets and sources (Price et al., 2015).

Fig. 2. Representative views of intestinal villi in *Eptesicus fuscus* (top row), *Microtus pennsylvanicus* (middle row), and *Atelerix albiventris* (bottom row). Left to right, sections from the proximal, medial, and distal thirds of the intestine are shown. The bar shows 100 μm.

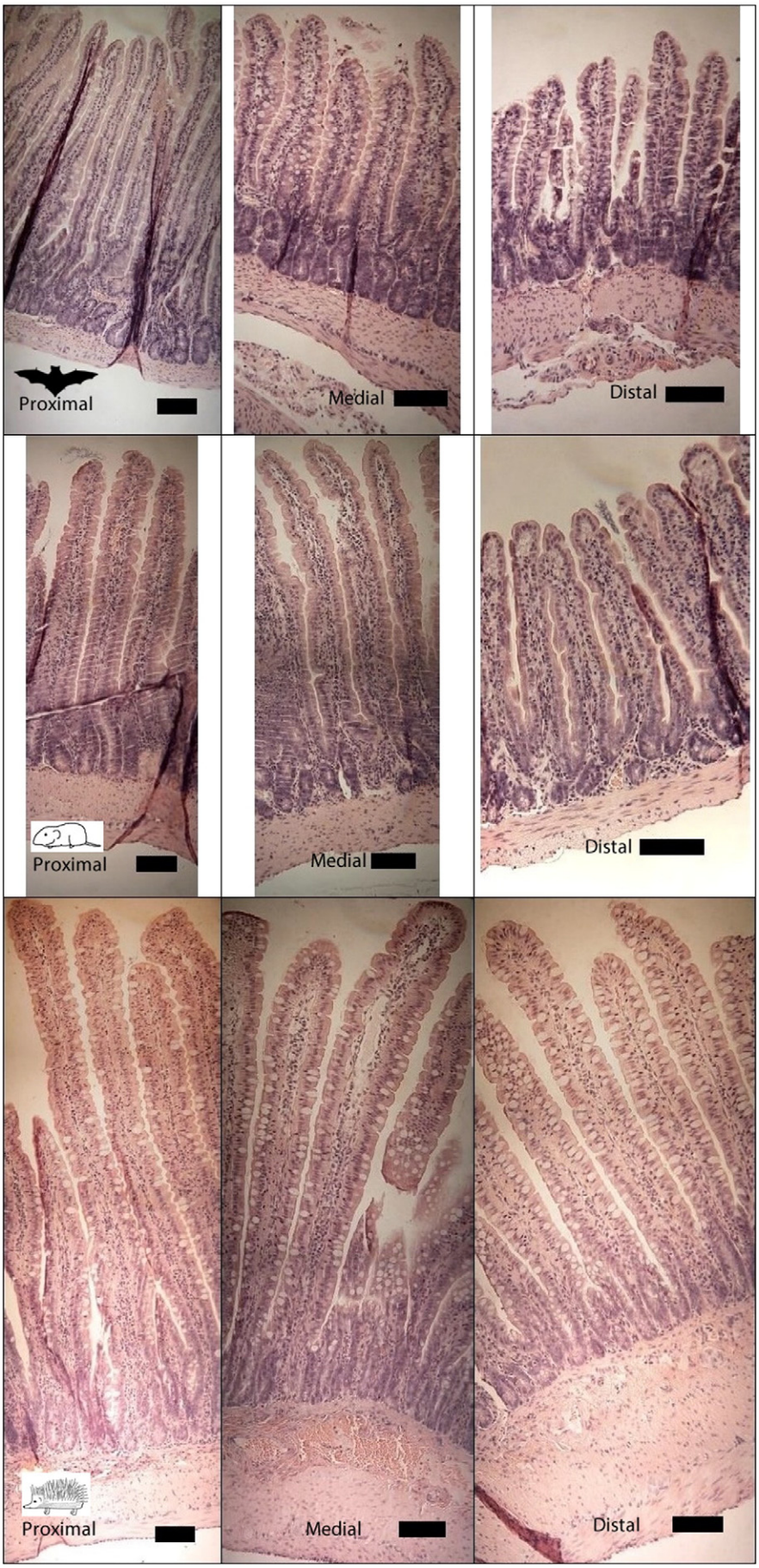
Proximal
Medial
Distal
Proximal
Medial
Distal
Proximal
Medial
Distal

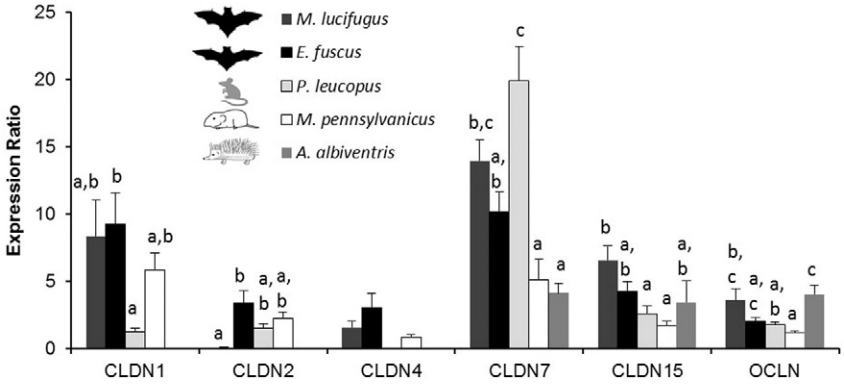

Fig. 3. Expression ratios of several claudins (CLDN) and occludin (OCLN) in the intestine of 2 bats, 2 rodents, and a hedgehog. Expression ratio is presented as the ratio of target gene expression to expression of ZO-1. Expression was not measured in the hedgehog (*A. albiventris*) for CLDN1, CLDN2, and CLDN4, nor in *P. leucopus* for CLDN4. For a given gene, bars sharing similar letters do not differ significantly ($P > 0.05$). $N_{M.\ lucifugus} = 9$, $N_{E.\ fuscus} = 11$, $N_{P.\ leucopus} = 8$, $N_{M.\ pennsylvanicus} = 9$, $N_{A.\ albiventris} = 6$. Data on *M. lucifugus* and *P. leucopus* are recalculated from Price et al. (2014). Data are means + SE.

Due to the size-sieving effect of tight junctions, absorption of larger molecules is inhibited (Delahunty and Hollander, 1987; Bijlsma et al., 1995; Chediack et al., 2003; Anderson and Van Itallie, 2009; Fasulo et al., 2013b). Because of this, and the size differential between L-arabinose (M_r 150) and D-glucose (M_r 180), our measurement of L-arabinose absorption overestimates the paracellular portion of glucose absorption. Nonetheless, our measurements show distinct differences among species in the paracellular absorption of nutrient-sized molecules, and this very likely extends to glucose as well.

4.2. Histological measurements

The high level of L-arabinose absorption in bats could potentially derive from having more tight junctions across which L-arabinose can absorb. Compared to the voles and hedgehogs, big brown bats have shorter and narrower intestines, i.e., the bats have a smaller nominal surface area (the surface area considering the intestine a smooth-bore tube). This could potentially be offset by greater villous amplification or enterocyte density in the bats. However, while the bats had somewhat smaller (and therefore more densely packed) enterocytes than either of the non-flyers, villous amplification was similar in the bats and voles, and even higher in the hedgehogs. Thus, for a given quantity of nominal surface area, bats and hedgehogs had a similar number of enterocytes, and presumably, tight junctions. Although the number of cells per nominal surface area was greater in the bats than in the voles, when we take into account the greater surface area of the voles, the total number of enterocytes in the small intestine is greater in voles than bats. Moreover, the total number of enterocytes in hedgehog small intestine was approximately 10 fold greater than the bats. When controlling for the effect of body mass on nominal surface area, bats had more total enterocytes than the vole but not the hedgehog. However, the proximate factors controlling absorption of paracellular probes should be the permeability of individual tight junctions, the absolute number of tight junctions, and the transit time, the latter of which was not measured here but is generally much faster in bats (Klite, 1965; Buchler, 1975; Price et al., 2015) than non-flyers. Bats cannot, therefore, obtain their high rates of paracellular nutrient absorption simply by having more junctions between cells through which the nutrients can be absorbed.

4.3. mRNA expression of tight junction-associated genes

An alternative mechanism for explaining the high level of paracellular nutrient absorption in bats is that the tight junctions of bats are somehow more permeable to nutrient-sized molecules. While it is unclear what characteristics determine tight junction permeability to nutrients, it is thought that the relative expression of the proteins that form the tight junction – CLDNs and OCLN – could be responsible (Günzel and Yu, 2013). We therefore investigated the expression of several tight junction genes that are known to be highly expressed in the small intestine (Holmes et al., 2006). For this, we focused on the ratios of expression of the several CLDNs and OCLN to expression of ZO-1, so as to control for any differences among species in the number of tight junctions per sampled tissue. This should have the effect of comparing among species the relative amount of each CLDN or OCLN expressed per tight junction.

The patterns of gene expression we observed in these 3 species, in combination with those previously reported (Price et al., 2014), did not demonstrate a clear difference between bats and non-flying mammals. We previously reported that the bat *M. lucifugus* had higher CLDN1 expression than the cricetid mouse *P. leucopus* (Price et al., 2014). While CLDN1 could not be measured in hedgehogs, its expression ratio in the vole was similar to that in both bat species. We also reported a low expression ratio of CLDN2 in *M. lucifugus* relative to *P. leucopus* (Price et al., 2014), but the CLDN2 expression ratio was much higher in the bat *E. fuscus*, and was similar to that of the vole. We did observe a replication of the pattern in CLDN15, to the extent that both bats had (non-significantly) higher CLDN15 expression ratios than both rodents. However, the hedgehog had a CLDN15 expression ratio similar to the bats, and therefore there was not a general difference between the flyers and non-flyers. The principal components analysis confirmed these findings. The five species had substantial overlap on their PC axes, and the 2 bats did not form a coherent and distinct group apart from the non-flyers.

Although these data do not support the hypothesis that interspecific differences in paracellular nutrient absorption are determined by the composition of claudins in the tight junction, we caution several caveats. We only measured expression at a single point along the intestine. If expression patterns vary considerably along the length of the intestine (Holmes et al., 2006), or if the point we chose is not analogous among species, then our data may not be easily comparable across species. Additionally, the composition of tight junctions, in terms of proteins present, may differ from gene expression patterns due to differences in translation and protein catabolism, as well as shuttling of proteins between tight junctions and intracellular pools (Shen et al., 2008, 2011).

4.4. Methodological considerations

Gene expression is most commonly compared within a species across treatments. This design allows certain assumptions in the methodology. These include assumptions that the fluorescence per amplicon is constant and that the reaction efficiency is constant, at least within a range of starting concentrations. Our cross-species design necessitated

Table 4
Factor loadings for the first two axes of a principal components analysis of tight junction gene expression.

	PC1	PC2
Proportion explained	0.368	0.293
Factor loadings:		
Cldn1/ZO1	0.892	−0.575
Cldn2/ZO1	−1.2279	−0.717
Cldn4/ZO1	−1.1777	−0.984
Cldn7/ZO1	0.594	−0.612
Cldn15/ZO1	0.231	−1.375
Ocln/ZO1	1.118	−0.7573

evaluation of these assumptions and/or adjustments for deviations. When possible, we designed primers that could be used to amplify genes in several species. This methodological step alone should largely satisfy both assumptions, because reaction efficiency is primarily a function of primer binding, and similar-length amplicons of the same gene should have similar fluorescence. Using the same primers for multiple species also has the advantage of being able to use a single mastermix for all samples.

When different primer sets are necessary, adjustments must be made for both the fluorescence per amplicon and the reaction efficiency. Determining the fluorescence per amplicon is perhaps the most difficult aspect. While amplicon length affects the fluorescence of Sybr Green, it is not clear exactly why this is. Sybr Green exhibits both intercalation and surface binding to DNA (Zipper et al., 2004). The increase in fluorescence with increasing amplicon length has been found to be driven mostly by adenine–thymine (AT) content (Zipper et al., 2004; Colborn et al., 2008), but contrasting studies attribute the most of the increase in fluorescence to guanine–cytosine (GC) content (Giglio et al., 2003; Gudnason et al., 2007). The fact that various studies have found opposing results suggests that SYBR Green binding/fluorescence may vary with specific DNA sequences. In light of this possibility, we believe our practice of using total amplicon length (which will also tend to correlate with other variables such as AT content and GC content) is the best way to normalize among different amplicons. As further confirmation of the robustness of our results, normalizing using AT content instead of total amplicon length would not have changed our conclusions (data not shown). We also note that our conclusions would be substantially similar even if we had restricted our analysis to only the 3 new species of this study, which all had quite similar amplicons.

An additional consideration when comparing across species is the choice of an appropriate denominator gene to form an expression ratio. We used ZO-1 as our primary denominator gene to assess the compositional makeup of the tight junctions. This choice was based primarily on the idea that using a ratio of two tight junction genes should control for any among-species differences in tight junctions, and thus, this ratio should reflect the proportion that any particular claudin or occludin makes up in the tight junction. Alternatively, we could have used standard reference genes, such as the EEF1A1 and RPLP0 that we measured, in the denominator. Using ratios based on standard reference genes should reflect the amount of each claudin per tissue that was sampled, which would be affected by both the abundance of the claudin in each tight junction and the total number of tight junctions. This might give results that are difficult to interpret if, for example, species varied in the amount of muscular or connective tissue per amount of epithelial layer. In our data, we would have come to similar conclusions using either denominator (compare Fig. 3 with Fig. S7), although the pattern of gene expression would be slightly different. The similarity of these two results may serve as confirmation that ZO-1 is constitutively expressed in tight junctions, or might indicate that our species have a fairly similar ratio of tight junctions to total intestine.

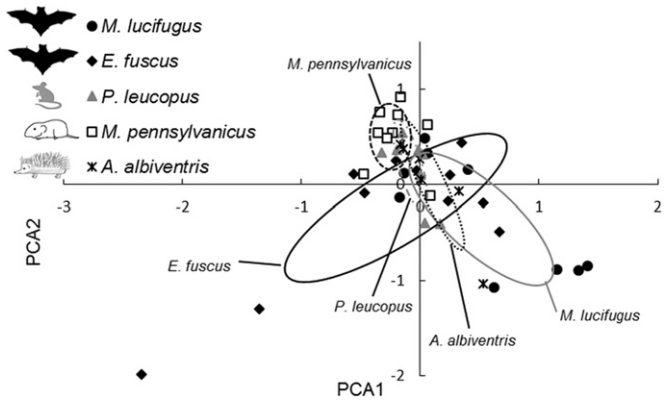

Fig. 4. Principal components analysis of gene expression ratios of several claudins and occludin in the intestine of 2 bats, 2 rodents, and a hedgehog. The first principal component is plotted on the horizontal axis and the second principal component is plotted on the vertical axis. Ellipses are 95% confidence ellipses for each species.

5. Conclusions

In agreement with previous studies, the big brown bat absorbed much more of an L-arabinose dose than either the vole or hedgehog. This difference cannot be explained by the bat having more enterocytes, and presumably more tight junctions, in their intestines; in fact, hedgehogs have 10-fold more enterocytes than the bat. The differences in paracellular permeability of the intestine to nutrient-sized molecules are therefore likely mediated by differences in the permeability of the tight junctions in the various species. Our gene expression profiles of tight junction-associated genes failed to detect a consistent pattern of expression differences between bats and non-flyers, although a larger dataset or measurements of protein abundance might yet shed more light on this problem.

Supplementary data to this article can be found online at http://dx.doi.org/10.1016/j.cbpb.2015.09.003.

Acknowledgments

We thank Jim Gammeter, Jerry Goth (Swamp Lover's Conservancy), Zach DeQuattro, the UW Lakeshore Nature Preserve, and the City of Madison Parks Division for providing access to lands and trapping assistance. Zach Peery graciously shared his lab equipment. Cherry Tsai provided laboratory assistance and we thank Becky Kirby for helpful discussions of reaction efficiency. We thank Chelsea Magruder for her mouse image. An anonymous reviewer provided helpful comments on the manuscript. Funding was provided by the National Science Foundation (IOS-1025886 to WHK and ECV) and the Department of Forest and Wildlife Ecology at the University of Wisconsin-Madison.

Appendix A

After correction for background fluorescence (Ruijter et al., 2009), the equation relating the fluorescence at threshold (F_t) to the number of starting copies (N_0) is

$$F_t = N_0 \cdot E^{Ct} \cdot S, \quad (1)$$

where E = reaction efficiency, with range [1,2]; C_t = cycle count when the fluorescence threshold is reached; and S = fluorescence per single copy of the amplicon. Rearranging,

$$N_0 = F_t / \left(E^{Ct} \cdot S\right) \quad (2)$$

With typical qPCR, in which differences in expression are measured within a species, S is dropped in practice. This is because it is an

unknown quantity, and because it is a constant across treatments, and therefore is not necessary for calculating "fold difference". For example, the fold difference of individual 1 versus individual 2 is:

$$N_{0(1)}/N_{0(2)} = \left\{F_t/\left(E^{Ct(1)}\cdot S\right)\right\}/\left\{F_t/\left(E^{Ct(2)}\cdot S\right)\right\} = E^{Ct(2)}/E^{Ct(1)} = E^{\{Ct(2)-Ct(1)\}} \quad (3)$$

The LinRegPCR program (Ruijter et al., 2009), for example, presents starting concentrations as:

$$N_{0LinRegPCR} = F_t/E^{Ct} \quad (4)$$

However, the primers and amplicons of different species (denoted here by species A, B, etc.) may differ in both E and S. We can chose to set F_t equal for both species, and we can calculate E for each species individually. For example, for species A, Eq. 4 will now be calculated:

$$N_{0LinRegPCR} = F_t/{E_A}^{Ct}, \quad (5)$$

where E_A is the reaction efficiency for species A. However, we must still account for interspecific differences in S. Here, we assume S for species A is a function of the length of the amplicon for species A and a fluorescence constant k_F that describes the fluorescence of SYBR Green when bound to double-stranded DNA. This k_F is invariant across amplicons. Thus,

$$S_A = Length_A \cdot k_F, \quad (6)$$

where $Length_A$ = the amplicon length for species A. Measuring expression for species A then derives from substituting Eq. 5 into Eq. 2 while making it specific to species A:

$$N_0 = N_{0LinRegPCR}/S_A \quad (7)$$

Substituting using Eq. 6

$$N_0 = N_{0LinRegPCR}/\{Length_A \cdot k_F\} \quad (8)$$

Because k_F is constant across amplicons, we can drop it for all subsequent calculations of fold difference or expression ratios. Thus we simplify to our final equation

$$N_0 = N_{0LinRegPCR}/Length_A. \quad (9)$$

References

Amasheh, S., Meiri, N., Gitter, A.H., Schöneberg, T., Mankertz, J., Schulzke, J.D., Fromm, M., 2002. Claudin-2 expression induces cation-selective channels in tight junctions of epithelial cells. J. Cell Sci. 115, 4969–4976. http://dx.doi.org/10.1242/jcs.00165.

Anderson, J.M., Van Itallie, C.M., 2009. Physiology and function of the tight junction. Cold Spring Harb. Perspect. Biol. 1, a002584. http://dx.doi.org/10.1101/cshperspect.a002584.

Benson, D.A., Karsch-Mizrachi, I., Clark, K., Lipman, D.J., Ostell, J., Sayers, E.W., 2012. GenBank. Nucleic Acids Res. 40, D48–D53. http://dx.doi.org/10.1093/nar/gkr1202.

Bijlsma, P.B., Peeters, R.A., Groot, J.A., Dekker, P.R., Taminiau, J.A., Van Der Meer, R., 1995. Differential in vivo and in vitro intestinal permeability to lactulose and mannitol in animals and humans: a hypothesis. Gastroenterology 108, 687–696.

Brody, T., 1999. Nutritional Biochemistry. Academic Press, San Diego.

Brun, A., Price, E.R., Gontero-Fourcade, M.N., Fernandez-Marinone, G., Cruz-Neto, A.P., Karasov, W.H., Caviedes-Vidal, E., 2014. High paracellular nutrient absorption in intact bats is associated with high paracellular permeability in perfused intestinal segments. J. Exp. Biol. 217, 3311–3317.

Buchler, E.R., 1975. Food transit time in *Myotis lucifugus* Chiroptera: Vespertilionidae. J. Mammal. 56, 252–255.

Caviedes-Vidal, E., Karasov, W.H., Chediack, J.G., Fasulo, V., Cruz-Neto, A.P., Otani, L., 2008. Paracellular absorption: a bat breaks the mammal paradigm. PLoS One 3, e1425. http://dx.doi.org/10.1371/journal.pone.0001425.

Caviedes-Vidal, E., McWhorter, T.J., Lavin, S.R., Chediack, J.G., Tracy, C.R., Karasov, W.H., 2007. The digestive adaptation of flying vertebrates: high intestinal paracellular absorption compensates for smaller guts. Proc. Natl. Acad. Sci. U. S. A. 104, 19132–19137.

Chediack, J.G., Caviedes-Vidal, E., Fasulo, V., Yamin, L.J., Karasov, W.H., 2003. Intestinal passive absorption of water-soluble compounds by sparrows: effect of molecular size and luminal nutrients. J. Comp. Physiol. B. 173, 187–197. http://dx.doi.org/10.1007/s00360-002-0314-8.

Colborn, J.M., Byrd, B.D., Koita, O.A., Krogstad, D.J., 2008. Estimation of copy number using SYBR Green: confounding by AT-rich DNA and by variation in amplicon length. Am. J. Trop. Med. Hyg. 79, 887–892.

Delahunty, T., Hollander, D., 1987. A comparison of intestinal permeability between humans and three common laboratory animals. Comp. Biochem. Physiol. A Comp. Physiol. 86, 565–567.

Fasulo, V., Zhang, Z., Chediack, J.G., Cid, F.D., Karasov, W.H., Caviedes-Vidal, E., 2013a. The capacity for paracellular absorption in the insectivorous bat *Tadarida brasiliensis*. J. Comp. Physiol. B. 183, 289–296. http://dx.doi.org/10.1007/s00360-012-0696-1.

Fasulo, V., Zhang, Z., Price, E.R., Chediack, J.G., Karasov, W.H., Caviedes-Vidal, E., 2013b. Paracellular absorption in laboratory mice: molecule size-dependent but low capacity. Comp. Biochem. Physiol. Part A. 164, 71–76.

Giglio, S., Monis, P.T., Saint, C.P., 2003. Demonstration of preferential binding of SYBR Green I to specific DNA fragments in real-time multiplex PCR. Nucleic Acids Res. 31, e136.

Gudnason, H., Dufva, M., Bang, D.D., Wolff, A., 2007. Comparison of multiple DNA dyes for real-time PCR: effects of dye concentration and sequence composition on DNA amplification and melting temperature. Nucleic Acids Res. 35, e127.

Günzel, D., Yu, A.S.L., 2013. Claudins and the modulation of tight junction permeability. Physiol. Rev. 93, 525–569. http://dx.doi.org/10.1152/physrev.00019.2012.

Holmes, J.L., Van Itallie, C.M., Rasmussen, J.E., Anderson, J.M., 2006. Claudin profiling in the mouse during postnatal intestinal development and along the gastrointestinal tract reveals complex expression patterns. Gene Expr. Patterns 6, 581–588. http://dx.doi.org/10.1016/j.modgep.2005.12.001.

Karasov, W.H., 2012. Terrestrial vertebrates. In: Sibly, R.M., Brown, J.H., Kodric-Brown, A. (Eds.), Metabolic Ecology: A Scaling Approach. Wiley-Blackwell, Chichester, UK, pp. 212–224.

Karasov, W.H., Caviedes-Vidal, E., Bakken, B.H., Izhaki, I., Samuni-Blank, M., Arad, Z., 2012. Capacity for absorption of water-soluble secondary metabolites greater in birds than in rodents. PLoS One 7, e32417. http://dx.doi.org/10.1371/journal.pone.0032417.

Keegan, D.J., 1984. Glucose absorption in the fruit bat studied using the intestinal ring method (abstract). S. Afr. J. Sci. 80, 132.

Keegan, D.J., 1980. The lack of an active glucose transport system in the bat intestine (abstract). S. Afr. J. Sci. 76, 570–571.

Kisielinski, K., Willis, S., Prescher, A., Klosterhalfen, B., Schumpelick, V., 2002. A simple new method to calculate small intestine absorptive surface in the rat. Clin. Exp. Med. 2, 131–135.

Klite, P.D., 1965. Intestinal bacterial flora and transit time of three neotropical bat species. J. Bacteriol. 90, 375–379.

Kurta, A., Baker, R.H., 1990. *Eptesicus fuscus*. Mamm. Species 356, 1–10.

Larkin, M.A., Blackshields, G., Brown, N.P., Chenna, R., McGettigan, P.A., McWilliam, H., Valentin, F., Wallace, I.M., Wilm, A., Lopez, R., Thompson, J.D., Gibson, T.J., Higgins, D.G., 2007. Clustal W and Clustal X version 2.0. Bioinformatics 23, 2947–2948.

Lavin, S.R., McWhorter, T.J., Karasov, W.H., 2007. Mechanistic bases for differences in passive absorption. J. Exp. Biol. 210, 2754–2764. http://dx.doi.org/10.1242/jeb.006114.

Lindroth, R.L., Batzli, G.O., 1984. Food habits of the meadow vole (*Microtus pennsylvanicus*) in bluegrass and prairie habitats. J. Mammal. 65, 600–606.

McCarthy, K.M., Francis, S.A., McCormack, J.M., Lai, J., Rogers, R.A., Skare, I.B., Lynch, R.D., Schneeberger, E.E., 2000. Inducible expression of claudin-1-myc but not occludin-VSV-G results in aberrant tight junction strand formation in MDCK cells. J. Cell Sci. 113, 3387–3398.

Nery, M.F., González, D.J., Hoffmann, F.G., Opazo, J.C., 2012. Resolution of the Laurasian phylogeny: evidence from genomic data. Mol. Phylogenet. Evol. 64, 685–689.

Price, E.R., Brun, A., Caviedes-Vidal, E., Karasov, W.H., 2015. Digestive adaptations of aerial lifestyles. Physiology 30, 69–78.

Price, E.R., Rott, K.H., Caviedes-Vidal, E., Karasov, W.H., 2014. Paracellular nutrient absorption is higher in bats than rodents: integrating from intact animals to the molecular level. J. Exp. Biol. 217, 3483–3492.

Price, E.R., Ruff, L.J., Guerra, A., Karasov, W.H., 2013. Cold exposure increases intestinal paracellular permeability to nutrients in the mouse. J. Exp. Biol. 216, 4065–4070. http://dx.doi.org/10.1242/jeb.088203.

R Development Core Team, 2010. R: A Language and Environment for Statistical Computing.

Rozen, S., Skaletsky, H.J., 2000. Primer3 on the WWW for general users and for biologist programmers, in: Bioinformatics Methods and Protocols: Methods in Molecular Biology. Humana Press, Totowa, NJ pp. 365–386.

Ruijter, J.M., Rarakers, C., Hoogaars, W.M.H., Karlen, Y., Bakker, O., van den Hoff, M.J.B., Moorman, A.F.M., 2009. Amplification efficiency: linking baseline and bias in the analysis of quantitative PCR data. Nucleic Acids Res. 37, e45.

Santana, E.M., Jantz, H.E., Best, T.L., 2010. *Atelerix albiventris* (Erinaceomorpha: Erinaceidae). Mamm. Species 42, 99–110. http://dx.doi.org/10.1644/857.1.Key.

Schulzke, J.D., Gitter, A.H., Mankertz, J., Spiegel, S., Seidler, U., Amasheh, S., Saitou, M., Tsukita, S., Fromm, M., 2005. Epithelial transport and barrier function in occludin-deficient mice. Biochim. Biophys. Acta 1669, 34–42. http://dx.doi.org/10.1016/j.bbamem.2005.01.008.

Shen, L., Weber, C.R., Raleigh, D.R., Yu, D., Turner, J.R., 2011. Tight junction pore and leak pathways: a dynamic duo. Annu. Rev. Physiol. 73, 283–309. http://dx.doi.org/10.1146/annurev-physiol-012110-142150.

Shen, L., Weber, C.R., Turner, J.R., 2008. The tight junction protein complex undergoes rapid and continous molecular remodeling at steady state. J. Cell Biol. 181, 683–695.

Tamura, A., Hayashi, H., Imasato, M., Yamazaki, Y., Hagiwara, A., Wada, M., Noda, T., Watanabe, M., Suzuki, Y., Tsukita, S., 2011. Loss of claudin-15, but not claudin-2, causes Na + deficiency and glucose malabsorption in mouse small intestine. Gastroenterology 140, 913–923. http://dx.doi.org/10.1053/j.gastro.2010.08.006.

Tracy, C.R., McWhorter, T.J., Korine, C., Wojciechowski, M.S., Pinshow, B., Karasov, W.H., 2007. Absorption of sugars in the Egyptian fruit bat (*Rousettus aegyptiacus*): a paradox explained. J. Exp. Biol. 210, 1726–1734. http://dx.doi.org/10.1242/jeb.02766.

Van Itallie, C., Rahner, C., Anderson, J.M., 2001. Regulated expression of claudin-4 decreases paracellular conductance through a selective decrease in sodium permeability. J. Clin. Invest. 107, 1319–1327.

Zipper, H., Brunner, H., Bernhagen, J., Vitzthum, F., 2004. Investigations on DNA intercalation and surface binding by SYBR Green I, its structure determination and methodological implications. Nucleic Acids Res. 32, e103.